Electronic Raman scattering in the single-CuO_2 layered superconductor $Tl_2Ba_2CuO_{6+\delta}$

L. V. Gasparov
2. Physikalisches Institut, Rheinisch-Westfälische Technische Hochschull Aachen, 52056 Aachen, Germany and Institute for Solid State Physics, 142432, Chernogolovka, Moscow district, Russia

P. Lemmens and M. Brinkmann
2. Physikalisches Institut, Rheinisch-Westfälische Technische Hochschull Aachen, 52056 Aachen, Germany

N. N. Kolesnikov
Institute for Solid State Physics 142432, Chernogolovka, Moscow district, Russia

G. Güntherodt
2. Physikalisches Institut, Rheinisch-Westfälische Technische Hochschull Aachen, 52056 Aachen, Germany
(Received 21 May 1996)

Electronic Raman scattering in $Tl_2Ba_2CuO_{6+\delta}$ (Tl-2201) has been investigated in order to test whether the scattering cross section in high-temperature superconductors depends on the number of CuO_2 planes, i.e., sheets or specific details of the Fermi surface. The polarized Raman spectra have been measured in different scattering geometries for temperatures above and below T_c. The spectral features of Tl-2201 with one CuO_2 plane per unit cell are found to be similar to $Tl_2Ba_2Ca_2Cu_3O_{10}$ with three CuO_2 planes and those of other high-temperature superconductors with several CuO_2 planes per unit cell. The peak in the B_{1g} symmetry component of the scattering intensity is found at 460 cm^{-1} ($T_c=90$ K), or 430 cm^{-1} ($T_c=80$ K). The B_{1g} peak positions scale with T_c, and correspond to $2\Delta/k_BT_c=7.6\pm0.4$. The temperature dependence of the B_{1g} scattering component of Tl-2201 ($T_c=80$ and 90 K) reveals a deviation from BCS behavior. The experimental data are in qualitative agreement with the calculations of Devereaux and Einzel based on the $d_{x^2-y^2}$-wave symmetry of the order parameter used in the description of the Raman-scattering cross section. [S0163-1829(97)01101-6]

I. INTRODUCTION

Since the discovery of high-temperature superconductors (HTSC's), the pairing mechanism and the symmetry of the order parameter in these compounds are key questions at stake.[1,2] There are several experimental techniques which are able to address this problem. The experiments on quasiparticle tunneling,[3] the linear temperature dependence of the penetration depth,[4] the NMR and NQR measurements,[5,6] and angular-resolved photoemission experiments in $Bi_2Sr_2CaCu_2O_8$ (Refs. 7 and 8) have yielded results consistent with d-wave pairing. On the other hand, quasiparticle tunneling, the exponential temperature dependence of the penetration depth, as well as the measurements of the electronic Raman scattering in $Nd_{2-x}Ce_xCuO_4$ are consistent with s-wave pairing.[9–11] The measurements of the magnetic-field dependence of the dc superconducting quantum interference device (SQUID) (YBaCuO-Au-Pb arrangement)[12] clearly indicated d-wave behavior, while the experiments on single Josephson-junction Pb-Y-Ba-Cu-O (Ref. 13) showed s-type behavior. So while the experimental evidence in favor of d-wave symmetry of the order parameter continuously grows, there is still no final consensus about it.

Raman scattering is a potential tool to address the problem of the symmetry of the order parameter. It allows us to probe the symmetry of the scattering tensor by simply choosing different polarization directions of the incident and scattered light. From the investigations of the Raman scattering in conventional superconductors it is known that the superconducting transition manifests itself in a renormalization of the electronic Raman scattering intensity below T_c. It was found for Nb_3Sn and V_3Si (Refs. 14 and 15) that normalized Raman spectra of these compounds show for temperatures below T_c a peak associated with the pair-breaking process at the energy 2Δ, together with a strong decrease of the scattering intensity at frequencies lower than 2Δ. In high-temperature superconductors, the first measurements of electronic Raman scattering were reported in Refs. 16–19. But in this case the behavior of the electronic scattering differs from that in conventional superconductors: A pair-breaking peak develops in the spectra below T_c, but the scattering intensity at frequencies below 2Δ does not show the usual sharp decrease. Instead, a monotonic decrease toward zero frequency is found. Moreover, for different symmetry components (A_{1g}, B_{1g}, and B_{2g}) the renormalization of the scattering intensity for $T<T_c$ is different and they exhibit peaks at different frequencies.[18–27,29,30] These facts have been described by Devereaux *et al.*[26–28] in terms of $d_{x^2-y^2}$-wave pairing. Their calculations of the scattering cross section have been performed for a cylindrical single-sheeted Fermi surface in the framework of the kinetic equation approach. The symmetry of the crystal was taken into account through calculating the Raman vertex, which was expanded in terms of a complete set of crystal harmonics defined on the Fermi surface. It was found that nontrivial coupling between the Raman vertex and an assumed strongly anisotropic energy

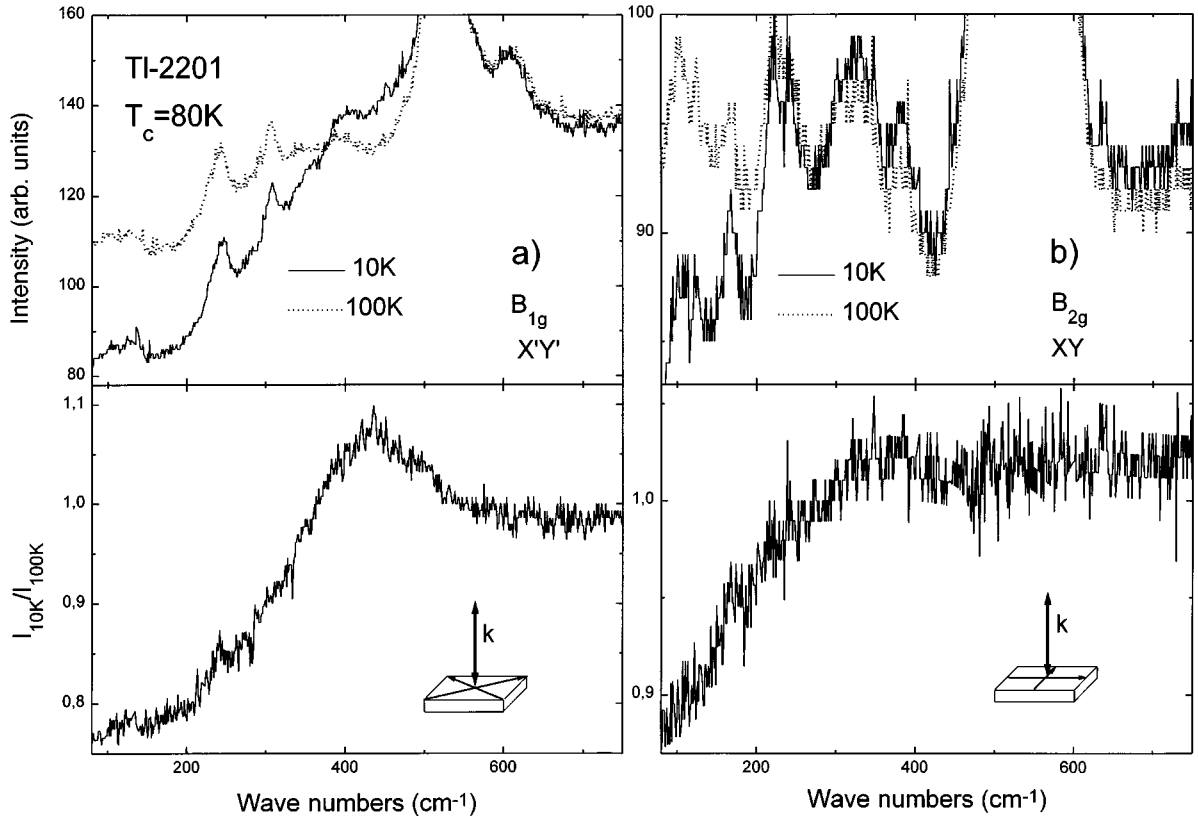

FIG. 1. Electronic Raman scattering of $Tl_2Ba_2CuO_{6+\delta}$ (T_c=80 K). Shown are spectra at T=10 and 100 K, and the divided spectra $I(T=10\ \mathrm{K})/I(T=100\ \mathrm{K})$ for (a) B_{1g} and (b) B_{2g} scattering components. The phonon at $\sim$490 cm^{-1} is due to the leakage of the A_{1g} scattering component, while the other phonons are defect-induced infrared-active phonons. Note that the peak in the divided spectrum does not coincide with the phonon at $\sim$490 cm^{-1}. The light polarization is shown in relation to the crystal axes.

gap leads to the strong symmetry dependence of the scattering intensity. The calculations[26,27] predict specific symmetry dependences of the low-frequency scattering as well as the peak positions for the different symmetry components of the electronic Raman scattering at temperatures below T_c. The A_{1g} peak position is sensitive to the parameters of the model calculation. It will appear below the B_{1g} peak position while with some parameters it may also appear at the B_{1g} peak position. Nevertheless there is one set of parameters which can reproduce the experimental data.[28] This model was criticized by Krantz and Cardona.[29,30] Their calculations[30] are based on the general description of the Raman-scattering cross section through the inverse effective-mass tensor. In case of the multisheeted Fermi surface (e.g., several CuO_2 planes per unit cell in HTSC's) polarization-dependent Raman efficiencies are determined by the averages of the corresponding effective-mass fluctuations. The authors of Ref. 30 used the effective masses from local-density approximation (LDA) band-structure calculations for $YBa_2Cu_3O_7$ to determine the Raman-scattering cross section. They found that it contradicts the experimental results if one uses only *d*-wave pairing for a multisheeted Fermi surface of $YBa_2Cu_3O_7$. An agreement was found by assuming different types of the order parameter on different sheets of the Fermi surface. For a single-sheeted Fermi surface (i.e., one CuO_2 plane per unit cell) the intraband mass fluctuations are strongly screened. Therefore in the framework of the effective-mass fluctuation approach, the A_{1g} scattering component will be nearly totally screened and should peak at the same position as the B_{1g} scattering component ($2\Delta_{\max}$). Therefore straightforward measurements of the electronic Raman scattering in single-CuO_2 layered high-temperature superconductors [Tl-2201, La-214, Bi-2201, (Nd,Ce)-214] should clarify this controversial point.

Tl-2201 has the highest T_c (up to 110 K) (Ref. 31) among the above-mentioned single-CuO_2 layered compounds. Therefore all effects due to the gap opening are expected in the range 300–600 cm^{-1}, and they should not be obscured due to the Rayleigh scattering at small wave numbers. Nevertheless, Raman measurements in only one pure scattering geometry (B_{1g}) are known[23,32] for this compound, which showed[23] besides a T_c=80 K two additional transitions at 100 and 125 K, which may be indicative of the Tl-2212 and Tl-2223 phases.

These facts lead us to reinvestigate the electronic Raman scattering in the Tl-based high-temperature superconductor Tl-2201 (with different oxygen content) with one CuO_2 plane per unit cell. The comparison with the results of electronic Raman-scattering experiments reported for the high-temperature superconductors with several CuO_2 planes should clarify whether the multiband scattering is indeed important. We should mention that similar experiments on the single layered compound (La-214) were already carried out.[25] Nevertheless, in the framework of a comparison of compounds with different numbers of CuO_2 planes the mea-

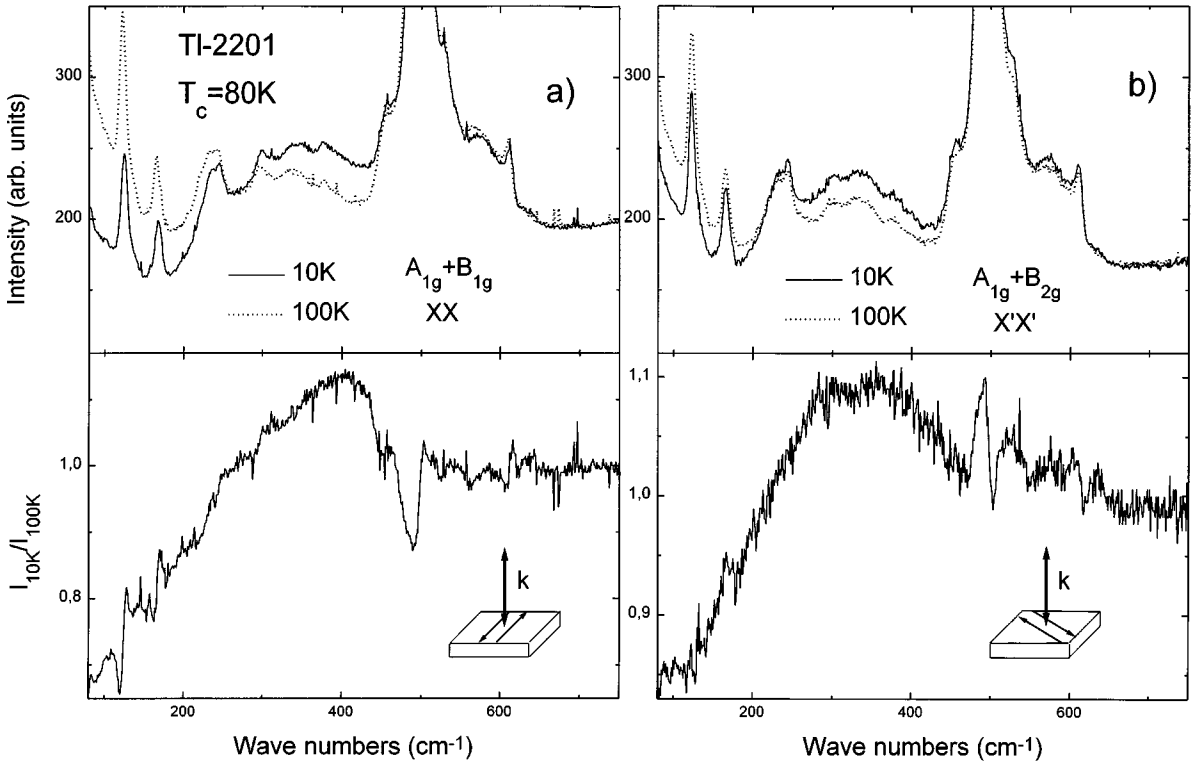

FIG. 2. Electronic Raman scattering of $Tl_2Ba_2CuO_{6+\delta}$ ($T_c=80$ K) in (a) $A_{1g}+B_{1g}(XX)$ and (b) $A_{1g}+B_{2g}(X'X')$ scattering geometries. Shown are spectra at $T=10$ and 100 K, and divided spectra $I(T=10\ \mathrm{K})/I(T=100\ \mathrm{K})$. The phonon at $\sim 490\ \mathrm{cm}^{-1}$ was cut off in order to show the variations of electronic Raman scattering. The polarization is shown in relation to the crystal axes.

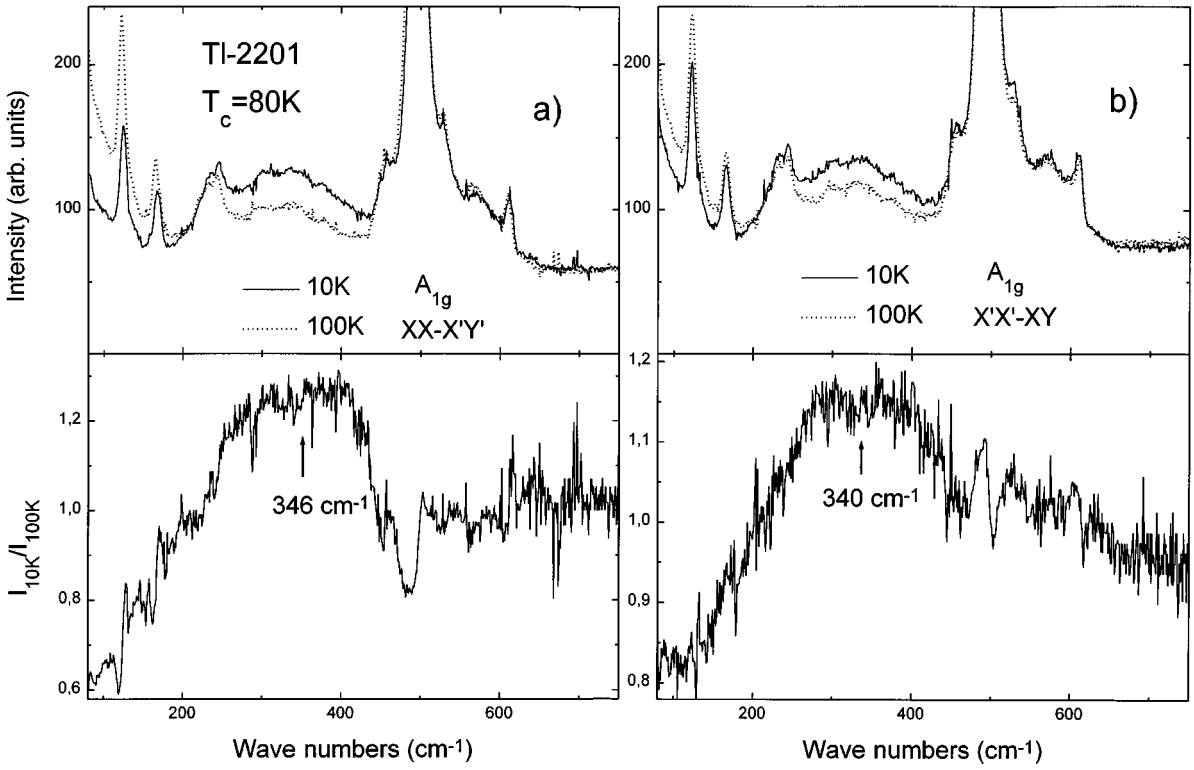

FIG. 3. Electronic Raman scattering of $Tl_2Ba_2CuO_{6+\delta}$ in A_{1g} scattering geometry evaluated from (a) XX and (b) $X'X'$ spectra. Shown are spectra at $T=10$ and 100 K, and divided spectra $I(T=10\ \mathrm{K})/I(T=100\ \mathrm{K})$. The phonon at $\sim 490\ \mathrm{cm}^{-1}$ was cut off in order to show the changes of electronic Raman scattering.

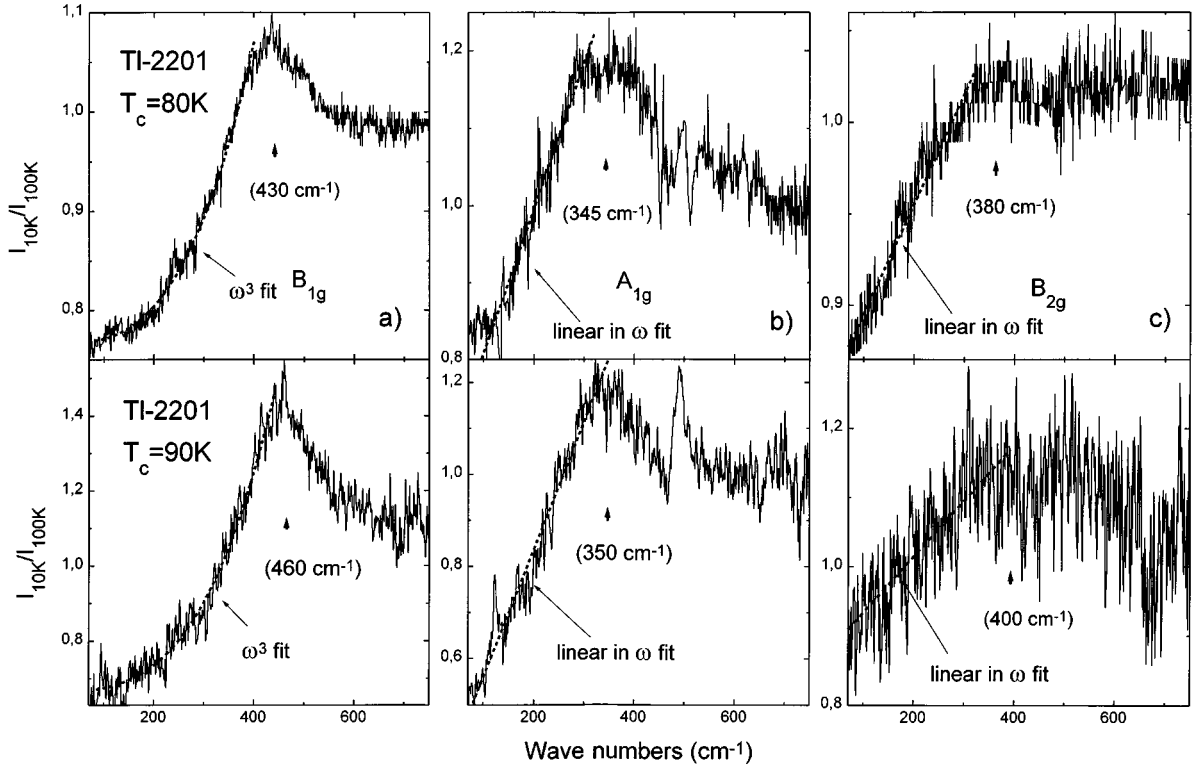

FIG. 4. Electronic Raman scattering in Tl-2201 with $T_c=80$ (upper panel) and 90 K (lower panel). Shown are divided spectra $I(T=10\ \mathrm{K})/I(T=100\ \mathrm{K})$ for (a) B_{1g}, (b) A_{1g}, and (c) B_{2g} scattering components.

surements on Tl-2201 are more favorable due to its high T_c.

II. EXPERIMENT

The investigated single crystals of $Tl_2Ba_2CuO_{6+\delta}$ (Tl-2201) had the shape of rectangular platelets with the size of approximately $2\times2\times0.2$ mm^3. The two crystals investigated were characterized by a SQUID magnetometer. T_c was found to be 90 ± 3 and 80 ± 5 K. The crystals are slightly underdoped. It is known[33] that differences in T_c in the Tl-2201 compound originate from different oxygen concentrations. These crystals can be over- as well as underdoped. The heavily oxygen doped crystals show a metallic type of conductivity[33] and do not show a superconducting transition. The orientation of the tetragonal crystals was controlled by x-ray diffraction.

Raman measurements were performed on ''as-grown'' surfaces of the freshly prepared crystals. This is very important, because the crystal surface of Tl-based superconductors as well as of all high-temperature superconductors is very sensitive to long exposure to air and especially to humid atmosphere. For the Raman measurements a DILOR XY triple spectrometer combined with a nitrogen-cooled CCD detector was used. All Raman data were obtained at nearly backscattering geometry. The photon excitation was provided by the 488-nm line of an Ar^+ ion laser with laser power equal to 15 W/cm^2. The estimated additional heating did not exceed 5 K.

III. EXPERIMENTAL RESULTS

All measurements were performed with the polarization of the incident and scattered light parallel to the basal plane of the crystal, i.e., the CuO_2 planes. It was possible to measure the A_{1g},B_{1g}, and B_{2g} symmetry components of the Raman-scattering cross section. In addition to the previously published phonon peaks ($\approx$123,$\approx$169,$\approx$490, $\approx$590,$\approx$610cm^{-1}),[34,35] we have detected some additional phonons ($\approx$240,$\approx$300,$\approx$330,$\approx$375cm^{-1}) which we believe are the defect-induced infrared-active phonons. For all scattering geometries the spectra for temperatures well below T_c were divided by the spectra just above T_c in order to emphasize the redistribution of the scattering intensity in the superconducting state compared to the normal state. The results of the electronic Raman scattering in the crystals of Tl-2201 (T_c=80,90 K) are shown in Figs. 1–5. In the crystal with $T_c=80$ K the B_{1g} scattering component measured in the $X'Y'$ configuration shows a well-defined peak at 430 ± 15 cm^{-1} [Fig. 1(a)]. The X' and Y' axes are rotated by 45° with respect to the crystal X and Y axes, respectively, which are parallel to the crystallographic axes. The B_{2g} scattering component in Fig. 1(b) is less intense, but shows also a broad maximum with an average frequency of 380 ± 35 cm^{-1}. Raman spectra in the XX and $X'X'$ geometries are presented in Figs. 2(a) and 2(b), showing spectra of $A_{1g}+B_{1g}$ and $A_{1g}+B_{2g}$ scattering components, respectively. In order to evaluate the A_{1g} scattering component we subtracted the B_{1g} and B_{2g} components [see Figs. 1(a) and 1(b)] from the XX and $X'X'$ spectra, respectively. As one can see from Figs. 3(a) and 3(b) the A_{1g} scattering component peaks for both scattering configurations, at 345 ± 20 cm^{-1}. For the crystal with $T_c=90$ K we found peaks of the B_{1g},A_{1g}, and B_{2g} scattering components at 460 ± 15, 350 ± 20, and 400 ± 35 cm^{-1}, respectively (Fig. 4, lower panel).

Another very important observation is that the low-

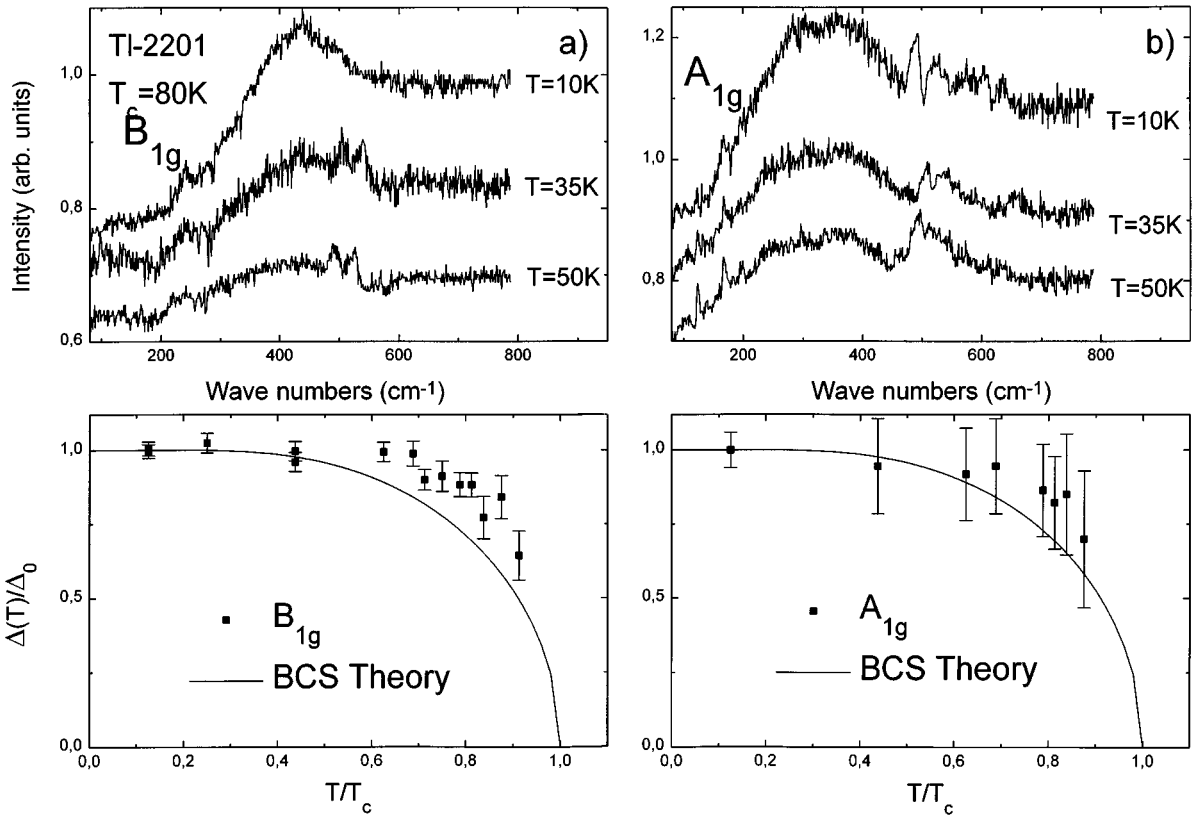

FIG. 5. Temperature dependence of the electronic Raman scattering. Shown are spectra for 10, 35, and 50 K (upper panel), and values of $\Delta(T)/\Delta_0$ (lower panel) evaluated for (a) B_{1g} and (b) A_{1g} scattering components. In the lower panel the temperature dependence of the peak positions is compared to that of the BCS theory.

frequency behavior of the electronic Raman scattering exhibits strong anisotropy with respect to the symmetry components. One can see in Fig. 4(a) (upper and lower panel) that the intensity decrease of the B_{1g} scattering component toward lower frequencies fits the ω^3 law predicted by Devereaux *et al.*[27] For the A_{1g} and B_{2g} scattering components in Figs. 4(b) and 4(c), respectively, there is a linear decrease, which also agrees with the predictions by Deveraux *et al.*[27] A summary of our results on Tl-2201 is presented in Table I.

In order to follow the temperature behavior of the superconductor gap, we have measured the temperature dependence of the electronic Raman scattering. Following Devereaux *et al.*,[26,27] we assume that the peak in the B_{1g} component of the electronic scattering corresponds to the value of $2\Delta_{\max}$. In Figs. 5(a) and 5(b), respectively, we show the B_{1g} and A_{1g} scattering component of Tl-2201 (T_c=80 K) at different temperatures between 10 K and T_c divided by the spectrum at 100 K. The experiments for the 90-K crystal yielded similar behavior.

With increasing temperature the intensity of the peak in Fig. 5(a) associated with the pair breaking process decreases and the maximum shifts slightly to lower frequencies. Obviously, the temperature dependence of the superconductor gap does not follow the BCS behavior. In other words, upon cooling below T_c the gap opens more abruptly than predicted by BCS theory. These results are similar to results reported for underdoped Bi-2212.[22] Because the peak position of the A_{1g} scattering component in Fig. 5(b) has larger error bars compared to the B_{1g} component, one cannot definitely say whether the data fit the BCS behavior or not.

We also searched for superconductivity-induced changes in frequency and linewidth of the optical phonons. With the resolution of 1 cm^{-1} we have not observed such changes. Upon heating from 10 up to 200 K the frequencies of all

TABLE I. Peak positions of the different scattering components of electronic Raman scattering. The reduced gap values $2\Delta/k_BT_c$ are referred to the B_{1g} peak position, n is the number of CuO_2 planes per unit cell.

Compound	n	T_c (K)	B_{1g} (cm^{-1})	A_{1g} (cm^{-1})	B_{2g} (cm^{-1})	$2\Delta/k_BT_c$
$Tl_2Ba_2CuO_6$	1	90	460±15	350±20	400±35	7.4±0.4
$Tl_2Ba_2CuO_6$	1	80	430±15	345±35	380±35	7.8±0.4

phonons decreased and the linewidths increased monotonically.

IV. DISCUSSION

The Raman-scattering intensity can be written in terms of the differential scattering cross section:[27]

$$\frac{\partial^2\sigma}{\partial\omega\partial\Omega}=\frac{\omega_s}{\omega_i}r_0^2 S_{\gamma\gamma}(\vec{q},\omega) \tag{1}$$

with

$$S_{\gamma\gamma}(\vec{q},\omega)=-\frac{1}{\pi}[1+n(\omega)]\Im m\chi_{\gamma\gamma}(\vec{q},\omega). \tag{2}$$

Here $r_0=e^2/mc^2$ is the Thomson radius, $\omega_i(\omega_s)$ is the frequency of incident (scattered) photon, $\hbar$ and k_B were set to 1. $S_{\gamma\gamma}$ is the generalized structure function, which is connected to the imaginary part of the Raman response function $\chi_{\gamma\gamma}$ through the fluctuation-dissipation theorem; $n(\omega)=1/[\exp(\omega/T)-1]$ is the Bose-Einstein distribution function. The Raman response function can be written as[36]

$$\chi_{\gamma\gamma}(\vec{q},\omega)=\langle\gamma_{\vec{k}}^2\lambda_{\vec{k}}\rangle-\frac{\langle\gamma_{\vec{k}}\lambda_{\vec{k}}\rangle^2}{\langle\lambda_{\vec{k}}\rangle} \tag{3}$$

with the Raman vertex $\gamma_{\vec{k}}$ written as

$$\gamma_{\vec{k}}(\omega_i,\omega_s)=\sum_L \gamma_L(\omega_i,\omega_s)\Phi_L(\vec{k}), \tag{4}$$

where $\Phi_L(\vec{k})$ are either Brillouin-zone or Fermi-surface harmonics[27] which transform according to point-group transformations of the crystal and $\lambda_{\vec{k}}$ is the Tsuneto function:

$$\lambda_{\vec{k}}\propto\frac{|\Delta_{\vec{k}}|^2}{\omega\sqrt{\omega^2-4|\Delta_{\vec{k}}|^2}}. \tag{5}$$

The brackets $\langle\cdots\rangle$ in Eq. (3) denote an average of the momentum $\vec{k}$ over the Fermi surface.

As is obvious, Raman scattering probes only $|\Delta|^2$. Therefore it is not possible to determine whether the gap function changes sign for different directions of $\vec{k}=(k_x,k_y)$ or not. But nevertheless the symmetry of the order parameter can be inferred from the specific spectral features of each symmetry component of the electronic Raman scattering.

For the gap of d-wave symmetry ($\Delta_{\vec{k}}=\Delta_{\max}\cos2\phi$, where ϕ is an angle between $\vec{k}$ and the a axis), calculations[26,27] predict different low-frequency behavior for the different symmetry components. For B_{2g} and A_{1g} scattering components it should show a linear dependence in ω, but for B_{1g} it should be $\sim\omega^3$. The appearance of a power law in the low-frequency scattering characterizes an energy gap which vanishes on the Fermi surface. The appearance of the ω^3 law in the B_{1g} scattering component is specific for $d_{x^2-y^2}$-wave pairing.[27] These above-mentioned peculiarities appear in our data. Indeed, the low-frequency behavior of the B_{1g} scattering component definitely differs from a linear behavior as seen in Fig. 4(a), whereas for the A_{1g} and B_{2g} scattering components it is linear in ω [see Figs. 4(b) and 4(c)]. For both crystals, the B_{1g} scattering component peaks at a higher frequency than the B_{2g}, which in turn peaks at a higher frequency than the A_{1g} component.

Since Raman scattering does not probe the phase of the order parameter it is important to take into consideration other types of the pairing which can also have nodes on the Fermi surface, but do not change the sign, i.e., $s+id$ pairing, or strongly anisotropic s pairing. For the $s+id$ pairing[27] [$\Delta(k)=\Delta_s+i\Delta_d\cos2\phi$] one gets the threshold at $\omega=2\Delta_s$ (minimum pair-breaking energy). While A_{1g} and B_{2g} scattering components exhibit a jump at this frequency, the B_{1g} scattering component shows a continuous rise from zero and up to the peak at $\omega=2\Delta_{\max}=2\sqrt{(\Delta_s^2+\Delta_d^2)}$. The A_{1g} and B_{2g} scattering components also show broad maxima as in the case of pure $d_{x^2-y^2}$-wave pairing, but these maxima will be cutoff toward lower frequencies due to the strong jump at $2\Delta_s$. Thus one should observe a low-frequency cutoff in both A_{1g} and B_{2g} scattering components, which, however, is not observed in our data.

For anisotropic s pairing, showing the minimum of the gap on the diagonals of the two-dimensional Brillouin zone, [$\Delta(k)=\Delta_0+\Delta_1\cos^4 2\phi$] one gets a single threshold on $2\Delta_0$ for all scattering components as well as a peak at $\omega=2\Delta_{\max}=2(\Delta_0+\Delta_1)$ for the B_{1g} scattering component. Therefore we will expect a picture which is very similar to the case of $s+id$ pairing, with one exception. The B_{1g} scattering component should show an additional shoulder at the same position where the A_{1g} and B_{2g} scattering components show peaks.[27] This is also not the case for our data. In principle, one can assume Δ_0 to be very small or even zero. In this case one gets peaks at $2\Delta_{\max}$,$0.6\Delta_{\max}$, and $0.2\Delta_{\max}$ for the B_{1g},B_{2g}, and A_{1g} scattering components,[27] respectively. In addition, the low-frequency behavior of the B_{1g} scattering component will be linear. This also contradicts our results.

Recently the model calculations of Devereaux *et al.* were criticized by Krantz and Cardona.[29,30] The main argument against this theoretical model is that the realistic electronic band structure of the crystal is important, but that the one-sheeted Fermi-surface approximation used by Devereaux *et al.* [27] is inappropriate. The authors of Ref. 30 used a numerical model based on the LDA band-structure calculations for YBaCuO in order to take into account the multisheeted Fermi surface of the superconductors with several CuO_2 planes. It was pointed out that for the $\Delta=\Delta_0\cos2\phi$ (d-wave pairing) and a multisheeted Fermi surface the calculations lead to a contradiction with the experiment, i.e., the A_{1g} and B_{1g} scattering components peak at the same position $2\Delta_0$. In order to get consistency with the experiment, different types of the order parameter on different sheets of the Fermi surface were proposed. Only in this case the calculations in Ref. 30 were able to get different positions of the maxima of the B_{1g},A_{1g}, and B_{2g} scattering components. For a single-sheeted Fermi surface the authors of Ref. 30 found almost identical positions of the maxima for the A_{1g} and B_{1g} components, but a different position for the B_{2g} compo-

TABLE II. Interplanar Cu-Cu distance and dimpling (Cu-O-Cu angle in CuO_2 plane) for different high-temperature superconductors with two ($n=2$) CuO_2 planes per unit cell.

Compound	n	T_c (K)	Interplane distance (Å)	Dimpling (deg)
$YBa_2Cu_3O_{7-\delta}$ (Ref. 40)	2	92	3.37	164
$TlBa_2CaCu_2O$ (Ref. 41)	2	103	3.20	177
$Tl_2Ba_2CaCu_2O_8$ (Ref. 42)	2	110	3.17	178
$Bi_2Sr_2CaCuO_8$ (Ref. 43)	2	84	3.44	179
$La_{1.6}Sr_{0.4}CaCu_2O_{5.94}$ (Ref. 44)	2	55	3.40	175

nent. Hence it was suggested that any difference in peak position of the A_{1g} and B_{1g} component is only consistent with multiband scattering of a multisheeted Fermi surface and different gap symmetries for each of the sheets. For superconductors with one CuO_2 plane, a multisheeted Fermi surface is invoked originating from Tl-like s states[30] (Tl-2201) or from Sr doping[37] ($La_{2-x}Sr_xCuO_4$) in order to yield a difference in peak position for the A_{1g} and B_{1g} components. However, no experimental proof for such a Fermi-surface contribution exists so far. Moreover, the calculations in Ref. 30 failed in explaining the symmetry-dependent low-frequency dependence of the Raman-scattering intensity, whereas this important experimental fact was observed not only in our experiments, but also in Bi-Sr-Ca-Cu-O,[21,22,26] Y-Ba-Cu-O,[18,19] and La-Sr-Cu-O (Ref. 25) systems. In addition, it is obvious that all superconductors with different crystal structures have a different electronic structure. Hence, if the multiband scattering model would be crucial we would expect absolutely different behavior for the different superconductors which is actually in contradiction with existing experimental results. Even if one compares the superconductors with the same number of CuO_2 planes, one finds that, while the interplanar distance (distance between Cu atoms in different CuO_2 planes) is quite similar, the dimpling (in-plane Cu-O-Cu angle) differs very much from compound to compound (see Table II). $YBa_2Cu_3O_7$ exhibits the largest dimpling compared to other compounds. Dimpling strongly affects the LDA calculations because the interplanar interaction depends on this parameter.

And finally on top of that, use of the effective-mass approach in addressing absolute scattering intensities[37] is questionable in the case of high-temperature superconductors, because this approach can be used only for nonresonant Raman scattering.[38] In high-temperature superconductors we, however, are always in the regime of the resonant scattering. Moreover, the electron correlation effects in HTSC's are not treated correctly by LDA.

In contrast to the conclusion of Ref. 30 our experiments show that the one-CuO_2-plane compound Tl-2201 shows very similar behavior compared to compounds with several CuO_2 planes, such as Tl-2223, Bi-2212, and YBaCuO.[18–27,29,30] We also found that the frequency of the B_{1g} maximum scales with T_c, and it corresponds to the value $2\Delta_{\max}/k_BT_c=7.6\pm0.4$. This value is very close to the values [with the exception of $Nd_{2-x}Ce_xCuO_4$ (Ref. 11)] found for other high-temperature superconductors as shown in Table III.

The temperature dependence of the gap [B_{1g} component in Fig. 5(a)] in our experiment differs from the BCS behavior, i.e., upon cooling the gap opens more abruptly than predicted by BCS theory. This is consistent with the spin-fluctuation theory of high-temperature superconductivity,[39] favoring $d_{x^2-y^2}$-wave pairing. The model considers pair binding as well as pair-breaking effects due to the spin fluctuations. Gap opening leads to a suppression of low-frequency spin fluctuations and therefore to reduced pair breaking. Therefore in underdoped crystals (our Tl-2201 crystals are underdoped) this effect will lead to a more abrupt opening of the gap upon cooling below T_c compared to BCS behavior.

In conclusion, we presented measurements of the electronic Raman scattering on high-T_c Tl-2201 single crystals with one CuO_2 plane per unit cell. The peculiarities of the electronic Raman scattering, i.e., the power-law frequency dependence of the different scattering components at low

TABLE III. Peak positions of the different symmetry components and reduced gap values $2\Delta/k_BT_c$ for different investigated high-temperature superconductors with different number n of CuO_2 planes per unit cell.

Compound	n	T_c (K)	B_{1g} (cm^{-1})	A_{1g} (cm^{-1})	$2\Delta/k_BT_c$
$YBa_2Cu_3O_{7-\delta}$ (Ref. 24)	2	89.7	420	310	7.6
		93.7	550	310	8.4
$Bi_2Sr_2CaCuO_8$ (Ref. 22)	2	81	460	280	8.2
		86	520	330	8.7
$La_{2-x}Sr_xCuO_4$ (Ref. 25)	1	37	200	125	7.8
$Tl_2Ba_2Ca_2Cu_3O_{10}$ (Ref. 20)	3	118	610	430	7.5
$Nd_{2-x}Ce_xCuO_4$ (Ref. 11)	1	19.3	70	70	5.2

frequencies, their different peak positions as well as the values of $2\Delta_{max}/k_BT_c = 7.6 \pm 0.4$ are found to be very similar in compounds with one and several CuO_2 planes. All nearly optimally doped high-T_c superconductors [with the exception of (Nd,Ce)-214 (Ref. 11)] show very similar behavior of the electronic Raman scattering consistent with the $d_{x^2-y^2}$-wave symmetry of the underlying order parameter.

ACKNOWLEDGMENTS

This work was supported by DFG through SFB 341 and by BMBF FKZ 13 N 6586. L.V.G. acknowledges support from the Alexander von Humboldt Foundation and expresses his gratitude for the hospitality at the 2.Physikalisches Institut RWTH-Aachen. We would like to thank M. Cardona and T. Strohm for a critical reading of the manuscript.

[1] R.C. Dynes, Solid State Commun. **92**, 53, (1994).
[2] J.R. Schrieffer, Solid State Commun. **92**, 129, (1994).
[3] J.M. Valles, Jr., R.C. Dynes, A.M. Cucolo, M. Gurvitch, L.F. Scneemeyer, J.P. Garno, and J.V. Waszczak, Phys. Rev. B **44**, 11 986 (1991).
[4] W.N. Hardy, D.A. Bonn, D.C. Morgan, R. Liang, and K. Zhang, Phys. Rev. Lett. **70**, 3999 (1993).
[5] Y. Kitaoka *et al.*, J. Phys. Chem. Solids **54**, 1385 (1993).
[6] C.P. Slichter *et al.*, J. Phys. Chem. Solids **54**, 1439 (1993).
[7] Z.Y. Shen, D.S. Dessau, B.O. Wells, D.M. King, W.E. Spicer, A.J. Arko, D. Marshall, L.W. Lombardo, A. Kapitulnik, P. Dickinson, S. Doniach, J. DiCarlo, A.G. Loeser, and C.H. Park, Phys. Rev. Lett. **70**, 1553 (1993).
[8] J. Ma, C. Quitmann, R.J. Kelley, H. Berger, G. Margaritondo, and M. Onellion, Science **267**, 862 (1995).
[9] N. Tralshawala, J.F. Zasadzinski, L. Koffey, and Q. Huang, Phys. Rev. B **44**, 12 102 (1991).
[10] S.N. Mao *et al.*, Appl. Phys. Lett. **64**, 375 (1994).
[11] B. Stadlober, G. Krug, R. Nemetschek, and R. Hackl, Phys. Rev. Lett. **74**, 4911 (1995).
[12] D.A. Wohlman, D.J. Van Harlinger, W.C. Lee, D.M. Ginsberg, and A.G. Leggett, Phys. Rev. Lett. **71**, 2134 (1993).
[13] A.G. Sun, D.A. Gajewski, M.B. Maple, and R.C. Dynes, Phys. Rev. Lett. **72**, 2267 (1994).
[14] R. Hackl, R. Kaiser, and S. Schicktanz, J. Phys. C **16**, 1729 (1983).
[15] S.B. Dierker, M.V. Klein, G.W. Webb, and Z. Fisk, Phys. Rev. Lett. **50**, 853 (1983).
[16] K.B. Lyons, M. Hong, H.S. Chen, J. Kwo, and T.J. Negrau, Phys. Rev. B **36**, 5592 (1987).
[17] A.V. Bazgenov *et al.*, in *Novel Superconductivity*, edited by S.A. Wolff and V.S. Kresin (Plenum, New York, 1987), p. 893; C. Thomsen, M. Cardona, R. Liu, B. Gegenheimer, and A. Simon, Physica C **153-155**, 1756 (1988).
[18] R. Hackl, W. Glaser, P. Müller, D. Einzel, and K. Anders, Phys. Rev. B **38**, 7133 (1988).
[19] S.L. Cooper, F. Slakey, M.V. Klein, J.P. Rice, E.D. Bukowski, and D.M. Ginsberg, Phys. Rev. B **38**, 11 934 (1988).
[20] A. Hofmann, P. Lemmens. G. Güntherodt, V. Thomas, and K. Winzer, Physica C **235-240**, 1897 (1994).
[21] T. Staufer, R. Nemetschek, R. Hackl, P. Müller, and H. Veith, Phys. Rev. Lett. **68**, 1069 (1992).
[22] A. Hoffmann, P. Lemmens, L. Winkeler, and G. Güntherodt, J. Low Temp. Phys. **99**, 201 (1995).
[23] R. Nemetschek, O.V. Misochko, B. Stadlober, and R. Hackl, Phys. Rev. B **47**, 3450 (1993).
[24] X.K. Chen, E. Altendorf, J.C. Irwin, R. Liang, and W.H. Hardy, Phys. Rev. B **48**, 10 530 (1993).
[25] X.K. Chen, J.C. Irwin, H.J. Trodahl, T. Kimura, and K. Kishio, Phys. Rev. Lett. **73**, 3290 (1994).
[26] T. Devereaux, D. Einzel, B. Stadlober, R. Hackl, D.H. Leach, and J.J. Neumeier, Phys. Rev. Lett. **72**, 396 (1994).
[27] T. Devereaux and D. Einzel, Phys. Rev. B **51**, 16 336 (1995).
[28] T. Devereaux and D. Einzel, Phys. Rev. B **54**, 15 547(E) (1996).
[29] M. Krantz and M. Cardona, Phys. Rev. Lett. **72**, 3290 (1994).
[30] M. Krantz and M. Cardona, J. Low Temp. Phys. **99**, 205 (1995).
[31] N.N. Kolesnikov, V.E. Korotkov, M.P. Kulakov, R.P. Shibaeva, V.N. Molchanov, R.A. Tamazyan, and V.I. Simonov, Physica C **195**, 219 (1992).
[32] G. Blumberg, M. King, P. Abbamonte, M.V. Klein, M. Karlow, S.L. Cooper, and N. Kolesnikov, Physica C **235-240**, 1137 (1994); C. Kendziora, R. J. Kelley, and M. Onellion, Proc. SPIE **2696**, 223 (1996).
[33] Y. Shimakawa, Physica C **202**, 199 (1992).
[34] L.V. Gasparov, V.D. Kulakovskii, O.V. Misochko, A.A. Polyanskii, and V.B. Timofeev, Physica C **160**, 147 (1989).
[35] M. Käll, L. Börjesson, C. Ström, S. Eriksson, and L.-G. Johansson, Physica C **220**, 131 (1994).
[36] M.V. Klein and S.B. Dierker, Phys. Rev. B **29**, 4976 (1984).
[37] M. Krantz (unpublished); T. Strohm and M. Cardona (unpublished); M. Cardona, T. Strohm, and J. Kircher, Proc. SPIE **2696**, 182 (1996).
[38] A.A. Abrikosov and V.M. Genkin, Sov. Phys. JETP **38**, 417 (1974).
[39] P. Monthoux, A.V. Balatsky, and D. Pines, Phys. Rev. B **46**, 14 803 (1992).
[40] J.D. Jorgensen, B.W. Veal, A.P. Paulikas, L.J. Nowicki, G.W. Crabtree, H. Claus, and W.K. Kwock, Phys. Rev. B **41**, 1866 (1990).
[41] B. Morosin, D.S. Ginley, P.F. Hlava, M.J. Carr, B.J. Baughman, J.E. Schirber, E.L. Venturini, and J.F. Kwak, Physica C **152**, 413 (1988).
[42] M.A. Subramanian, J.C. Calabrese, C.C. Torardi, J. Gopalakrishnan, T.R. Askew, R.B. Flippen, K.J. Morrissey, U. Chowdhry, and A.W. Sleight, Nature (London) **332**, 420 (1988).
[43] P. Bordet, J.J. Capponi, C. Chaillout, J. Chenavas, A.W. Hewat, E.A. Hewat, J.L. Hodeau, M. Marezio, J.L. Tholence, and D. Tranqui, Physica C **153-155**, 623 (1988).
[44] R.J. Cava, A. Santoro, J.J. Krajewski, R.M. Fleming, J.V. Wasczak, W.F. Peck, Jr., and P. Marsh, Physica C **172**, 138 (1990).